A Novel Electro-organic Synthesis of Pyrrolopyrazole Derivatives

Hussein M. Fahmy, Mohey E. Sharaf, and Mohammed A. Aboutabl
Department of Chemistry, Faculty of Science, Cairo University, Giza, A. R. Egypt
Mahmoud M. M. Ramiz and Magdi Abdel El-Azzem
Faculty of Electronic Engineering and Faculty of Science, El-Menoufia University, A. R. Egypt
Hassan Abd El-Rahman
General Metal Company, Giza, Helwan, A. R. Egypt

The polarographic reduction of two series of pyrazolone derivatives, namely ethyl 4-arylazo-5-oxo-4,5-dihydropyrazol-3-ylacetate derivatives (**1a–d**) and ethyl 4-arylazo-5-oxo-1-phenyl-4,5-dihydropyrazol-3-ylacetate derivatives (**2a–d**), is reported in detail for aqueous buffered media at a dropping mercury electrode (DME). Controlled-potential electrolysis (CPE) on four members showed that the products of electrolysis were ethyl 4-amino-5-oxo-4,5-dihydropyrazol-3-ylacetate (**5a**), 3,5-dioxo-2,3,3a,4,5,6-hexahydropyrrolo[3,2-*c*]pyrazole (**6a**), ethyl 4-amino-5-oxo-1-phenyl-4,5-dihydropyrazol-3-ylacetate (**5b**), and 3,5-dioxo-2-phenyl-2,3,3a,4,5,6-hexahydropyrrolo-[3,2-*c*]pyrazole (**6b**). These were isolated and identified through IR, ^{1}H NMR, and MS analyses. Also, the acid dissociation constants pK_{a1} and pK_{a2} were determined spectrophotometrically and a mechanism has been suggested and discussed for the electrode and ionization processes. Finally the results were shown to be predicted through Hammett correlations.

The chemistry and biological activity of pyrazole functionality fused to heterocyclic ring systems have attracted the attention of many workers, and this led to the synthesis of a variety of pyrazole derivatives exhibiting bacteriostatic, bactericidal, analgesic, and anti-inflammatory activities.[1–6] In the present work newly synthesized compounds, namely ethyl 5-oxo-4-phenylhydrazono-4,5-dihydro-1*H*-pyrazol-3-ylacetate (**1a–d**)

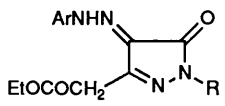

(**1**) R = H
(**2**) R = Ph

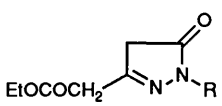

(**3**) R = H
(**4**) R = Ph

Ar
a; Ph
b; 4-ClC_6H_4
c; 4-MeC_6H_4
d; 4-$NO_2C_6H_4$

and ethyl 5-oxo-1-phenyl-4-phenylhydrazono-4,5-dihydro-1*H*-pyrazol-3-ylacetate (**2a–d**), have been studied polarographically in detail together with two model compounds, namely ethyl 5-oxo-4,5-dihydro-1*H*-pyrazol-3-ylacetate (**3**) and ethyl 5-oxo-1-phenyl-4,5-dihydro-1*H*-pyrazol-3-ylacetate (**4**).

Experimental

Light petroleum refers to the fraction boiling in the range 40–60 °C.

Organic Synthesis.—(i) *Synthesis of model compounds* (**3**) *and* (**4**). Ethyl 5-oxo-4,5-dihydro-1*H*-pyrazol-3-ylacetate (**3**) and ethyl 5-oxo-1-phenyl-4,5-dihydro-1*H*-pyrazol-3-ylacetate (**4**) were synthesized as previously described in the literature.[7]

(ii) *Synthesis of compounds* (**1a–d**) *and* (**2a–d**). A diazonium salt solution, prepared from the (*para*-substituted) aniline (0.01 mol) was added to an ice-cold solution of compound (**3**) and (**4**) (0.01 mol) in ethanol (20 cm^3) containing sodium acetate (2 g) and the mixture was left in an ice-bath for 1 h. The precipitated compound was collected, washed with water, and then recrystallized from the appropriate solvent (see Table 1).

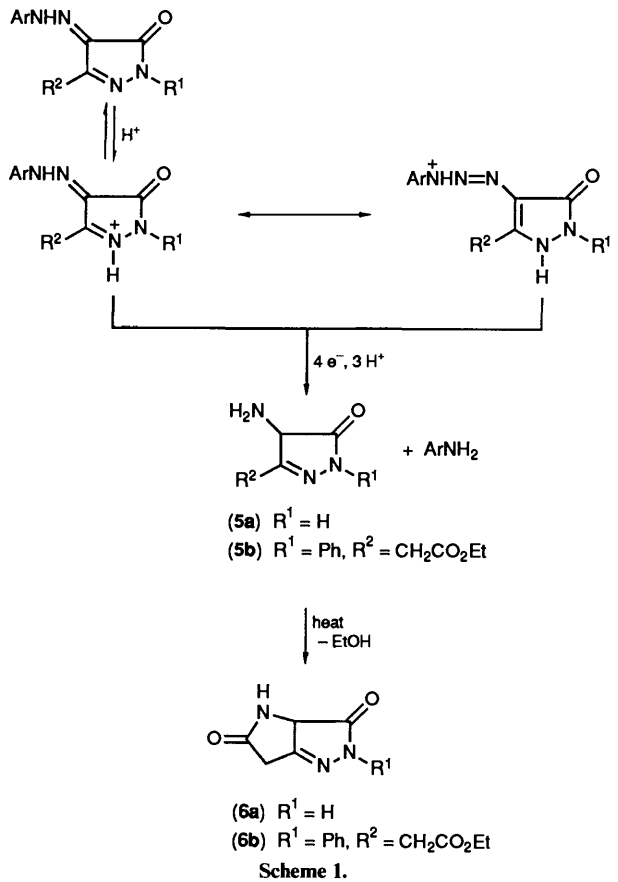

(**5a**) R^1 = H
(**5b**) R^1 = Ph, R^2 = CH_2CO_2Et

(**6a**) R^1 = H
(**6b**) R^1 = Ph, R^2 = CH_2CO_2Et

Scheme 1.

Instruments.—The *i–E* curves were recorded on a Tacussel PRT40 potentiostat, EPLI recorder, and PRG3 pilot. The cell was a Tacussel RMO4 cell. The capillary was a Tacussel

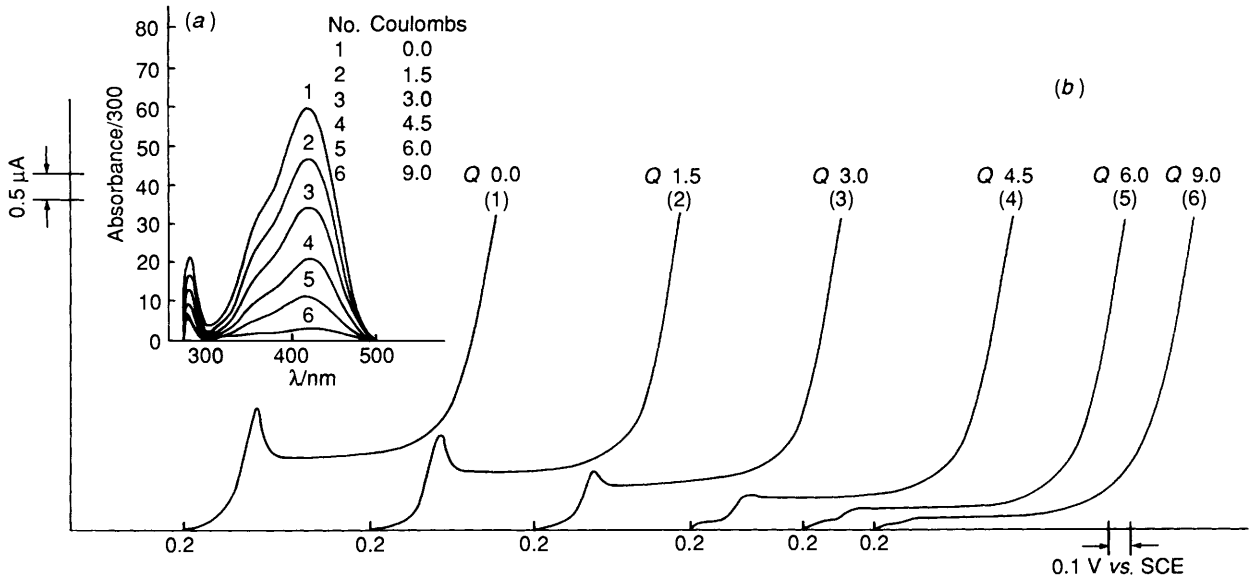

Figure 1. (*a*) Spectrophotometric follow-up curves at different intervals on electroreduction of compound (**1b**), number of coulombs are given on the plot. (*b*) CPE follow-up experiments, potential controlled at −0.65 V *vs.* SCE, Q-values are given on the polarograms in coulombs [compound (**1b**)].

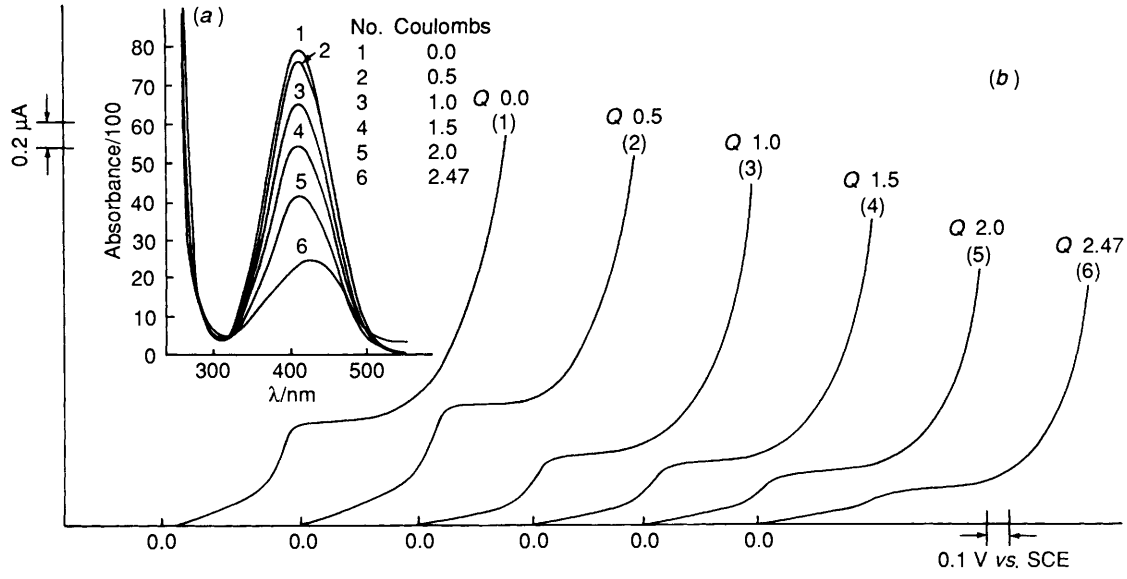

Figure 2. (*a*) Spectrophotometric follow-up curves at different intervals on electroreduction of compound (**2c**), number of coulombs are given on the plot. (*b*) CPE follow-up experiments, potential controlled at − 0.80 V *vs.* SCE, Q-values are given on the polarograms in coulombs [compound (**2c**)].

MTS124 (*m* 0.33 g s^{-1} for *h* 50 cm and controlled by a hammer with a frequency of 1 Hz). The number of electrons was computed with a Tacussel type IG3A electronic integrator in conjunction with the potentiostat. The absorption spectra were scanned on a PYE unicam 500 spectrophotometer within the wavelength range 200–550 nm. The IR spectra were recorded in KBr pellets on a Perkin-Elmer 397 instrument. The half-wave potentials are expressed *versus* standard calomel electrode (SCE) (with an accuracy of ±0.005 V) with a conventional three-electrode system.

Solutions and Procedures.—Stock solutions (10^{-3} mol dm^{-3}) were prepared by dissolving an accurately weighed quantity of material in the appropriate volume of absolute ethanol, Britton–Robinson buffers[8] were used as the supporting electrolyte, and ethanol (4 cm^3) and buffer solution (5 cm^3) were introduced into the cell. The mixture was then deaerated by bubbling a stream of oxygen through the solution for 10 min. The calculated amount of stock solution was then introduced into the cell so that the final concentration was 10^{-4} mol dm^{-3} 50% v/v ethanolic buffer (10 cm^3).

Follow-up Controlled-potential Electrolysis.—The follow-up experiments on 5 × 10^{-4} and 1.7 × 10^{-4} mol dm^{-3} ethyl 4-(4′-chlorophenylhydrazono)-5-oxo-4,5-dihydro-1*H*-pyrazol-3-ylacetate (**1b**) and ethyl 4-(4′-methylphenylhydrazono)-5-oxo-1-phenyl-4,5-dihydro-1*H*-pyrazol-3-ylacetate (**2c**) were carried out in acid medium, pH 1.5. The potential was fixed at −0.65 and −0.80 V, respectively, *i.e.* on the limiting current plateau of the wave. The electrolysis was followed by recording current–potential curves periodically together with spectrophotometric runs between 250–550 nm (see Figures 1 and 2). The actual number of electrons consumed during electrolysis was found to be 4.2 and 4.4 F mol^{-1} * for compounds (**1b**) and (**2c**),

* 1 F = *ca.* 9.648 × 10^4 C mol^{-1}.

Table 1. Data for compounds (**1a—d**) and (**2a—d**).

Compound	Molecular formula	M.p. /°C	Yield (%)	Analysis (%)	Required	Found
(**1a**)	$C_{13}H_{14}N_4O_3$	125	75	C	56.93	56.9
				H	5.11	5.1
				N	20.44	20.4
(**1b**)	$C_{13}H_{13}ClN_4O_3$	142	80	C	50.57	50.6
				H	4.21	4.2
				N	18.15	18.1
				Cl	11.51	11.5
(**1c**)	$C_{14}H_{16}N_4O_3$	116	80	C	58.33	58.3
				H	5.55	5.5
				N	19.44	19.3
(**1d**)	$C_{13}H_{13}N_5O_5$	124	80	C	48.90	48.9
				H	4.08	4.1
				N	21.94	21.8
(**2a**)	$C_{19}H_{18}N_4O_3$	118	80	C	65.14	65.1
				H	5.14	5.1
				N	16.00	16.0
(**2b**)	$C_{19}H_{17}ClN_4O_3$	136	82	C	59.30	59.3
				H	4.42	4.4
				N	14.56	14.5
				Cl	9.23	9.2
(**2c**)	$C_{20}H_{20}N_4O_3$	107	85	C	65.93	65.9
				H	5.49	5.5
				N	15.38	15.4
(**2d**)	$C_{19}H_{17}N_5O_5$	143	80	C	57.72	57.7
				H	4.30	4.3
				N	17.72	17.7

respectively. The UV spectra showed that the height of the bands at λ_{max} 425 and 420 nm decreased as the number of coulombs consumed increased. This can be taken as direct evidence that the reduction centre is the hydrazonic moiety.

Preparative Controlled-potential Electrolysis (CPE) *and Identification of the Resulting Products.*—(i) *CPE of compound* (**1b**). Compound (**1b**) (46 mg) was dissolved in 20% DMF–30% EtOH–50% HCl mixture (100 cm^3) (pH 1.95) and was electrolysed at a controlled potential of −0.65 V *vs.* SCE. After complete electrolysis the solution was evaporated to dryness under reduced pressure. The residue was then dissolved in a small amount of chloroform and chromatographed on a silica gel column with chloroform as the eluant, and a yellow product, ethyl 4-amino-5-oxo-4,5-dihydro-1*H*-pyrazol-3-ylacetate (**5a**), was obtained (≈15% yield), m.p. 200 °C; ν_{max}(KBr) 3 300–3 050 (NH), 1 730 (ester CO), 1 650 (C=O), and 1 470 cm^{-1} (C=N); δ_H[$(CD_3)_2SO$] 1.0 (3 H, t, Me), 2.6 (2 H, s, CH_2), 4.0 (2 H, q, CH_2), 5.1 (1 H, s, pyrazole 4-H), 8.3 (1 H, br s, NH), and 11.5 (2 H, br s, NH_2); *m/z* 185.

Reduction product 3,5-dioxo-2,3,3a,4,5,6-hexahydropyrrolo-[3,2-*c*]pyrazole (**6a**) was obtained with methyl alcohol as the eluant (≈65% yield), m.p. 105 °C (decomp.); ν_{max}(KBr) 3 100–2 850 (CH), 1 730 (ring C=O), 1 660 (ring C=O), and 1 580 (N=N); *m/z* 139; δ_H[$(CD_3)_2SO$] 6.1 (1 H, s, N=CH proton).

(ii) *CPE of compound* (**1c**). Electrolysis was carried out on compound (**1c**) (250 mg) in a mixture of EtOH (200 cm^3) and HCl (10 mol dm^{-3}; 20 cm^3) (pH 0.30). The potential was adjusted at −0.50 V *vs.* SCE. The progress of electrolysis was followed by recording the decay in current with time which started at 70 mA and dropped to 0.2 mA within 3 h. The resulting solution was evaporated to a fifth of its original volume. Then the solution was neutralized to pH ≈ 7.0 and an aliquot of the solution (10 cm^3) was removed from the mother liquor and tested for the presence of aniline by addition of β-naphthol. The remaining solution was in turn evaporated, and the precipitated product was recrystallized from ethyl alcohol (~70% yield). This product was identified as compound (**6a**) (Scheme 1).

(iii) *CPE of compound* (**2c**). The same procedure as described for the CPE of compound (**1b**) was carried out on compound (**2c**) (42 mg) in 30% DMF–30% EtOH–30% HCl mixture (90 cm^3) (pH 1.55). The potential was fixed at −0.80 V *vs.* SCE. The solution obtained was evaporated to dryness under reduced pressure and the residue was extracted with dichloromethane. The solution was chromatographed on a silica gel column with methyl alcohol as the eluant, and deep orange ethyl 4-amino-5-oxo-1-phenyl-4,5-dihydropyrazol-3-ylacetate (**5b**) was obtained (~20% yield), m.p. 210 °C; ν_{max} 3 600–3 100 (NH_2), 1 715 (ester CO), 1 650 (ring CO), and 1 600 cm^{-1} (C=N); δ_H[$(CD_3)_2SO$] 1.0 (3 H, t, Me), 2.6 (2 H, s, CH_2), 4.0 (2 H, q, CH_2), 5.1 (1 H, s, pyrazole 4-H), 7.1–7.7 (5 H, m, ArH), 8.3 (1 H, br s, NH), and 11.5 (2 H, br s, NH_2).

The insoluble product was washed several times with light petroleum and a deep red product, 3,5-dioxo-2-phenyl-2,3,3a,4,5,6-hexahydropyrrolo[3,2-*c*]pyrazole (**6b**), was obtained (~42% yield), m.p. 103 °C; ν_{max}(KBr) 3 000–2 850 (CH), 1 720 (ring CO), 1 650 (ring CO), and 1 580 cm^{-1} (N=N).

(iv) *CPE of compound* (**2a**). Mercury pool electrolysis was performed on a solution of compound (**2a**) (100 mg) in a mixture of EtOH (100 cm^3) and HCl (0.1 mol dm^{-3}; 100 cm^3) (pH 1.55). The potential was fixed at −0.45 V *vs.* SCE. At the beginning of electrolysis the current had a value of 80 mA and dropped to 0.1 mA at the end (8 h). The solution resulting from electrolysis was evaporated to a fifth of its original volume, then was neutralized to pH ~7.0, and an aliquot (10 ml) was removed to test in the presence of aniline (coupling with β-naphthol). The solution was evaporated and the isolated product was recrystallized from EtOH (~65% yield) to give compound (**6b**).

Spectrophotometry and Determination of pK_a*-Values.*—UV–visible spectrophotometry was carried out on 2 × 10^{-5} mol dm^{-3} solutions of the studied compounds in 50% v/v alcoholic Britton–Robinson buffer solution. Spectrophotometric measurements were recorded as a function of pH of solution. The pK_a was then calculated using the graphical correlation between pH and absorbance and by using the appropriate equations.[9] The absorbance–pH and log $(A - A_{min})/(A_{max} - A)$–pH plots of the two series (**1a–d**) and (**2a–d**) are illustrated in Figures 3 and 4.

It is clear that at each maximum (A_{max}) the absorption remains constant with increasing pH up to a definite pH-value

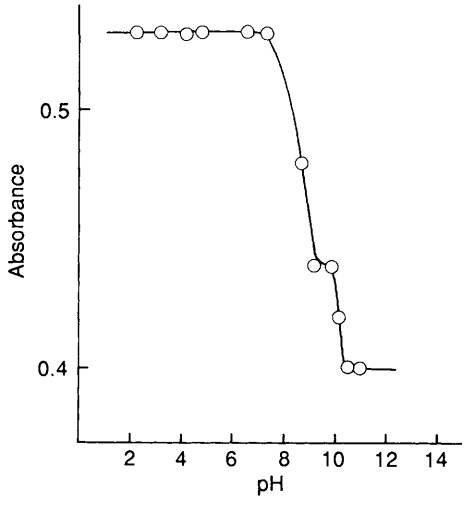

Figure 3. Absorbance–pH plot of 2 × 10^{-5} mol dm^{-3} compound (**1a**) in 50% (v/v) ethanolic Britton–Robinson buffers.

Table 2. Polarographic data for series (**1a–d**) (wave A).

Compound	$E_{\frac{1}{2}}$–pH	$RT^c/\alpha_n F$	α_n	pH[d]	pK_{a1}[e]	pK_{a2}[e]
(**1a**)	$E_{\frac{1}{2}} = -0.15 - 0.092$ pH[a]	0.035	1.69	2.70	8.55	10.10
	$E_{\frac{1}{2}} = -0.80 - 0.032$ pH[b]	0.066	0.90	7.80		
(**1b**)	$E_{\frac{1}{2}} = -0.13 - 0.086$ pH[a]	0.050	1.18	11.35		
	$E_{\frac{1}{2}} = -0.77 - 0.029$ pH[b]	0.044	1.34	2.99	8.90	10.35
(**1c**)	$E_{\frac{1}{2}} = -0.33 - 0.066$ pH[a]	0.050	1.18	7.00		
	$E_{\frac{1}{2}} = -0.62 - 0.04$ pH[b]	0.063	0.94	11.34		
(**1d**)	$E_{\frac{1}{2}} = -0.06 - 0.059$ pH[a]	0.030	1.97	2.26	8.35	10.25
	$E_{\frac{1}{2}} = -0.73 - 0.04$ pH[b]	0.032	1.85	7.95		
		0.033	1.79	12.00		
		0.033	1.79	2.70	7.40	10.50
		0.060	0.99	7.70		
		0.044	1.34	12.00		

[a] Equation of first segment. [b] Equation of second segment. [c] Slope from logarithmic analysis. [d] Individual pH-value at which logarithmic analysis was carried out. [e] Spectrophotometric acid dissociation constant.

Table 3. Polarographic data for series (**2a–d**) (wave A).

Compound	$E_{\frac{1}{2}}$–pH	$RT^c/\alpha_n F$	α_n	pH[d]	pK_{a1}[e]
(**2a**)	$E_{\frac{1}{2}} = -0.21 - 0.081$ pH[a]	0.042	1.41	2.56	6.95
	$E_{\frac{1}{2}} = -0.53 - 0.052$ pH[b]	0.042	1.41	7.70	
(**2b**)	$E_{\frac{1}{2}} = -0.19 - 0.073$ pH[a]	0.032	1.85	11.40	
	$E_{\frac{1}{2}} = -0.46 - 0.050$ pH[b]	0.026	2.27	2.81	6.60
(**2c**)	$E_{\frac{1}{2}} = -0.28 - 0.071$ pH[a]	0.031	1.91	8.05	
	$E_{\frac{1}{2}} = -0.074 - 0.03$ pH[b]	0.040	1.44	12.60	
(**2d**)	$E_{\frac{1}{2}} = -0.20 - 0.083$ pH[a]	0.033	1.79	2.76	8.30
	$E_{\frac{1}{2}} = -0.82 - 0.028$ pH[b]	0.031	1.91	8.20	
		0.025	2.36	12.06	
		0.033	1.79	3.65	7.4
		0.046	1.29	7.70	
		0.046	1.29	11.40	

[a] Equation of first segment. [b] Equation of second segment. [c] Slope from logarithmic analysis. [d] Individual pH-value at which logarithmic analysis was carried out. [e] Spectrophotometric acid dissociation constant.

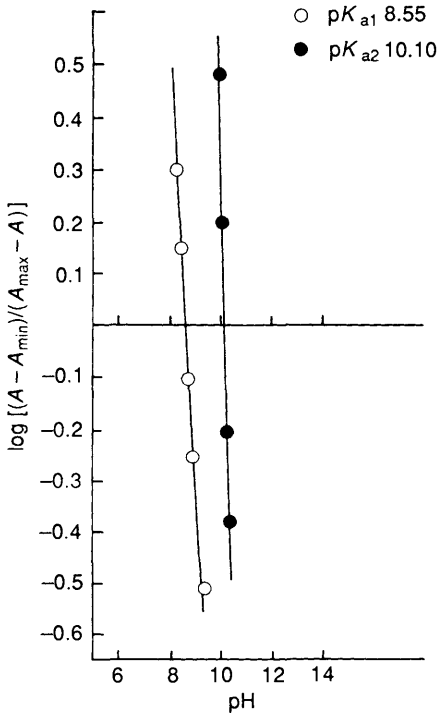

Figure 4. log $(A - A_{min})/(A_{max} - A)$–pH plot of 2×10^{-5} mol dm^{-3} compound (**1a**) in 50% (v/v) ethanolic Britton–Robinson buffers.

Table 4. Statistical treatment of pK_a–σ data for series (**1a–d**) and series (**2a–d**).

Hammett constants	ρ (1)	ρ (2)	r (1)	r (2)	sd (1)	sd (2)
σ	1.99	4.02	0.516	0.912	±0.642	±0.735
σ^0	2.00	3.61	0.555	0.875	±0.642	±0.735
σ^+	0.91	4.07	0.250	0.986	±0.642	±0.735

ρ = slope, r = correlation coefficient, and sd = standard deviation; (**1**) series (**1a–d**), (**2**) series (**2a–d**).

where it starts to decrease significantly to a minimum (A_{min}), at which the absorbance remains constant on further increase of solution pH increase. This function of absorbance with pH allows us to determine the acid–base equilibrium (K_a and hence pK_a). The obtained pK_a-values for both series are compiled in Tables 2 and 3

Results and Discussion

The polarograms of the parent compounds (**1a**) and (**2a**) (Figures 5 and 6) showed only one wave A at pH $< \sim 10$. Plots of $E_{\frac{1}{2}}$–pH showed one segment in which $E_{\frac{1}{2}}$ is sensitive to change in pH and another one practically pH-independent. The limiting current of wave A decreased with increasing pH in the form of a well-defined dissociation curve at pH $\geqslant$ pK_a. At pH > 10 another wave, B, appeared. The i_l of this latter wave increased with increasing pH. $E_{\frac{1}{2}}$ and i_l *versus* pH plots of waves A and B

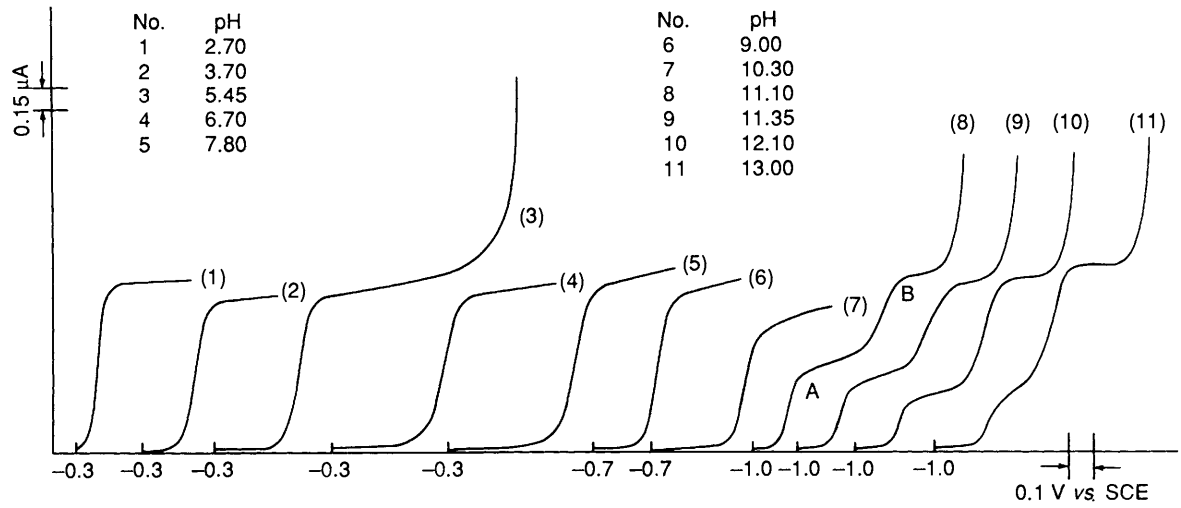

Figure 5. Polarograms of 10^{-4} mol dm^{-3} compound (**1a**) in 50% (v/v) ethanolic Britton–Robinson buffers. pH Given on the polarograms.

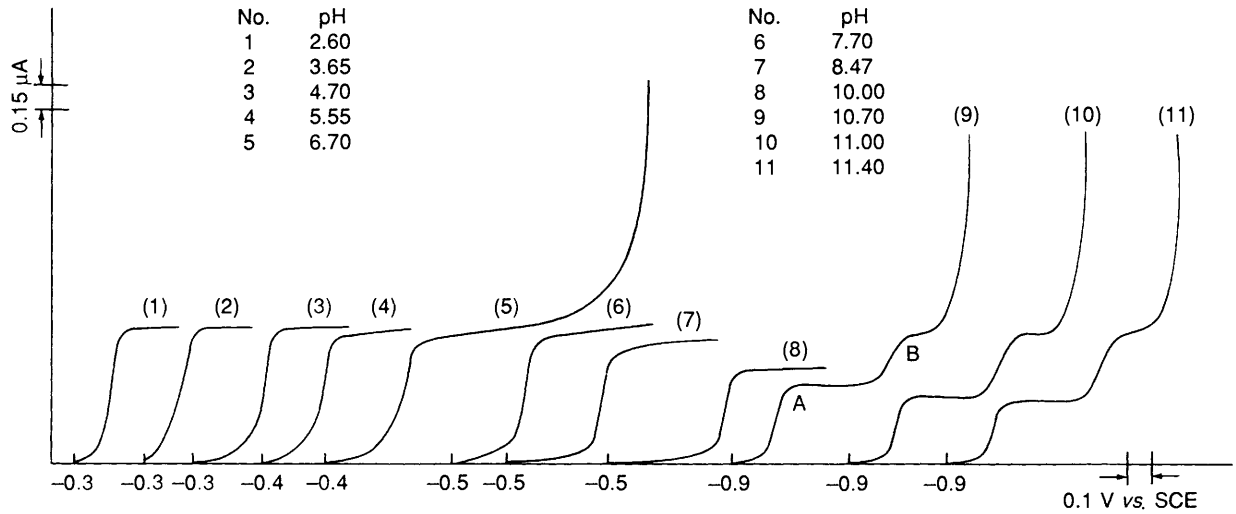

Figure 6. Polarograms of 10^{-4} mol dm^{-3} compound (**2a**) in 50% (v/v) ethanolic Britton–Robinson buffers. pH Given on the polarograms.

are shown in Figure 7. On the other hand the nitro derivative (**1d**) afforded one extra wave, C, for the classical reduction of the nitro group at a more positive potential as compared with waves A and B. The characteristic data for series (**1a–d**) are compiled in Table 2. Series (**2a–d**) showed similar behaviour to series (**1a–d**) (*cf.* Figures 6 and 7). The characteristic data for (**2a–d**) are compiled in Table 3.

Acid–Base Equilibrium and Mechanism of the Electrode Process.—It is necessary to recall the behaviour of series (**1a–d**) in which the hydrogen atom is linked to the N-1 nitrogen.

Substitution of the hydrogen atom in N-1 by a phenyl moiety (**2a–d**) will change the possible tautomerism, and hence pK_{a2}-values will be affected over the pH range studied. Also, it can be assumed that members of series (**1a–d**) are more acidic in nature than those of series (**2a–d**) (*cf.* Tables 2, 3), since the hydrogen atom linked to N-1 atom can also be located at the C=O or on N–NH as shown for the tautomeric forms in Scheme 2. By

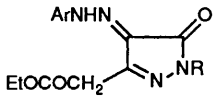

R = H for series (**1a–d**)
R = Ph for series (**2a–d**)

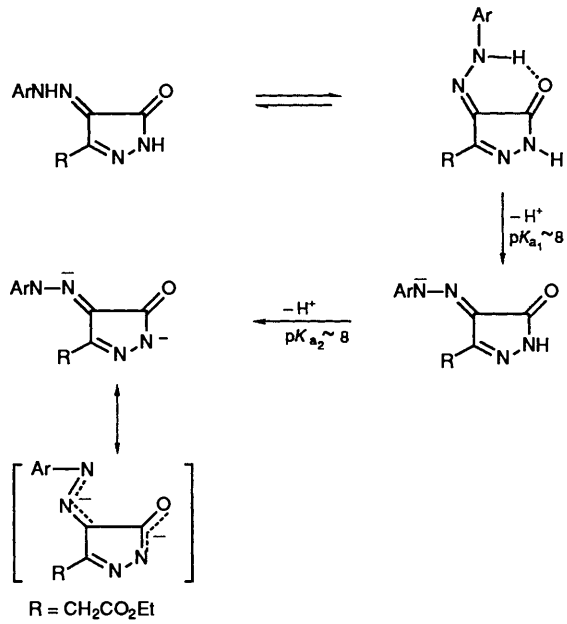

R = CH_2CO_2Et

Scheme 2.

Table 5. Statistical treatment of $E_{\frac{1}{2}}$–σ data (wave A) (**1a–d**) and (wave A) (**2a–d**).

	σ			σ^0			σ^+		
pH	ρ	*r*	sd	ρ	*r*	sd	ρ	*r*	sd
Series (**1a–d**)									
3	0.31	0.94	±0.054	0.35	0.94	±0.054	0.300	0.99	±0.054
7	0.16	0.65	±0.042	0.17	0.71	±0.042	0.120	0.28	±0.042
10.5	0.061	0.14	±0.074	0.09	0.22	±0.074	0.066	0.29	±0.074
Series (**2a–d**)									
3	0.17	0.96	±0.027	0.15	0.93	±0.027	0.16	0.98	±0.027
7	0.17	0.87	±0.032	0.16	0.91	±0.032	0.11	0.58	±0.032
11	0.17	0.60	±0.047	0.18	0.67	±0.047	0.06	0.22	±0.047

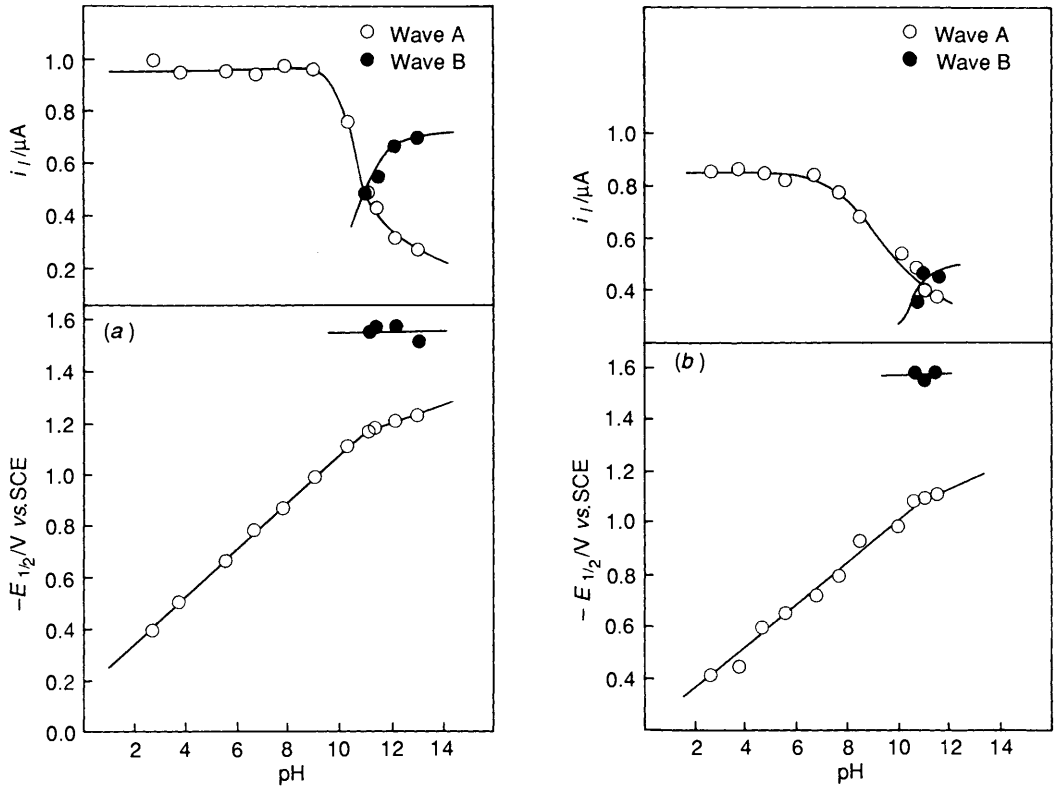

Figure 7. $E_{\frac{1}{2}}$– and i_l–pH plots for the polarographic waves [A]; compound (**1a**), [B]; compound (**2a**).

blocking this labile hydrogen through phenyl substitution at N-1, the C=O can now be involved in tautomerization only as represented by the following equilibrium. The pK_a-value for

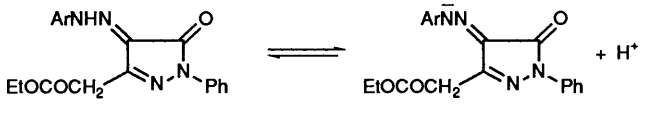

(2)

model compound (**3**) gave a value of *ca.* 8.0; this numerical value is lower than those obtained for series (**1a–d**) (pK_{a2}) (Tables 2, 3), since in series (**1a–d**) the ionization process actually involves the hydrazono NH–H hydrogen atom. Also, we should mention that model (**4**) gave no pK_a-value. From the foregoing results one can conclude that wave A is due to the reduction of the protonated form while wave B can be attributed to the reduction of the free base. Thus at pH < pK_a, the compound is reduced along a four-electron, irreversible, pH-dependent, diffusion-controlled wave A. At pH > pK_a, the free base is reduced along wave B. The segmentation of $E_{\frac{1}{2}}$–pH plots (Figure 7) indicates the participation of a proton in the acid–base equilibrium prior to the electro-reduction process itself.

According to the obtained results compiled in Tables 2 and 3, it is reasonable to assume a preprotonation of the molecule followed by its reduction in the sequence described in Scheme 1. It is important to mention that cyclization of compounds similar to products (**5a**) and (**5b**) is well known [10] so when we use moderate conditions to remove the solvent, the major product is the amino ester (**5a**) and (**5b**), while with evaporation and direct heating for a long period of time the cyclized (**6a**) and (**6b**) compounds were the main products obtained.

Finally it appeared necessary to study the effect of substituents on the reaction site of these molecules through pK_a and $E_{\frac{1}{2}}$–σ correlations. pK_a-Values obtained from spectrophotometric measurements are given in Tables 2 and 3. These values

were correlated against different σ constants through statistical treatment of the data using Jaffé calculations.[11] As is clear from Table 4, good linearity was obtained with slope values varying between 0.9–2.0 for series (**1a–d**) and ~4.0 for series (**2a–d**). These correlations indicate that the ionization centre is directly affected by the different substituents on the phenyl ring. The low values of the slope of the correlation of series (**1a–d**) as compared with the slope of series (**2a–d**) indicate that the ionization of the NH of the hydrazono linkage in series (**1a–d**) is counterbalanced by ionization of the N-1 hydrogen atom through the carbonyl group while in series (**2a–d**) the N-1 hydrogen atom has been exchanged by the phenyl moiety. On the other hand, the most reliable $E_{\frac{1}{2}}$-values at selected pH have been correlated with different Hammett σ constants.[12] As we have shown that linear plots with marked slopes are obtained at pH-values $\leqslant pK_a$, while at higher pH-values the correlations are poor, the $E_{\frac{1}{2}}$ values being almost independent of substituent, this can be explained by the fact that at high pH-values the molecules are in the ionized form.

References

1 M. J. Vitolo and E. V. Marquez, *J. Med. Chem.*, 1978, **21**, 692.
2 M. T. Di parsia, C. Swarez, M. J. Vitolo, and E. V. Marquez, *J. Med. Chem.*, 1981, **24**, 117.
3 M. M. Hashem and K. D. Berlin, *J. Med. Chem.*, 1976, **19**, 229.
4 F. Seidel, W. Thier, and A. Uber, *Chem. Ber.*, 1935, **688**, 1913.
5 S. Yasunoba, Y. Sato, Y. Shinneji, and H. Takagi, *Chem. Abstr.*, 1976, **84**, 16477m.
6 M. A. Khan, A. G. Cosenza, and G. P. Elles, *J. Heterocycl. Chem.*, 1982, **19**, 1077.
7 S. Kuo, L. Herang, and H. Nakamura, *J. Med. Chem.*, 1984, **27**, 539.
8 H. T. S. Britton, 'Hydrogen Ions,' Chapman and Hall, London, 4th edn., 1962, p. 313.
9 R. M. Issa and A. Z. Zawail, *J. Chem. U.A.R.*, 1971, **14**, 161.
10 H. Lund, *Acta Chem. Scand.*, 1964, **18**, 563.
11 H. H. Jaffé, *Chem. Rev.*, 1953, **53**, 191.
12 C. D. Ritchie and W. F. Sagar, *Prog. Phys. Org. Chem.*, 1964, **2**, 334.

Paper 0/00105H
Received 5th *January* 1990
Accepted 29th *April* 1990